Supporting Online Material

Thinning and flow of Tibetan crust constrained by seismic anisotropy

Nikolai M. Shapiro[1], Michael H. Ritzwoller[1], Peter Molnar[2], and Vadim Levin[3]

[1]Department of Physics, University of Colorado at Boulder, USA

[2]Department of Geological Sciences, Cooperative Institute for Research in Environmental Science (CIRES), University of Colorado at Boulder, USA

[3]Department of Geological Sciences, Rutgers University, New Jersey, USA

Data coverage and resolution

Surface-wave coverage for the Tibetan region (fig. S1) is denser at intermediate periods (~40 sec) than at longer periods. Intermediate periods are most sensitive to the Tibetan middle crustal structure. The average lateral resolution of the group velocity tomographic maps across the Tibetan region at those periods is about 200 km for both Rayleigh and Love waves.

Finding an optimal parameterization for Tibetan crustal structure

When inverting the surface-wave dispersion maps for the 3D shear velocity model we tested five different parameterizations for Tibetan crustal structure: two isotropic and three radially anisotropic. During those tests, we set the mantle structure to that obtained from a global inversion (1). The results of those five inversions (table S1) show that the parameterization with a radially anisotropic middle crust yields a root-mean-square misfit that is nearly half of the other parameterizations. Therefore, although we cannot eliminate a small amount of anisotropy in either the upper or the lower crust, we conclude that strong mid-crustal radial anisotropy is required to explain the observed surface-wave dispersion. During the final inversion, we selected the parameterization with a radially anisotropic middle crust and allowed the mantle structure to vary.

Relation between crustal thinning and radial anisotropy

We consider a horizontally isotropic crust flattened in its vertical direction using a strain tensor given by:

$$U = \begin{pmatrix} 1+\frac{\epsilon}{2} & 0 & 0 \\ 0 & 1+\frac{\epsilon}{2} & 0 \\ 0 & 0 & 1-\epsilon \end{pmatrix} \quad (1)$$

where ϵ is the amount of the crustal thinning. We consider a rock composed of mica crystals embedded in an isotropic matrix. In response to the vertical flattening, the mica crystals rotate

and become oriented more horizontally. Rotation of an individual mica crystal relative to the vertical axis can be considered as a two-dimensional problem where the crystal is represented by a position vector $\vec{r}$ and its deformation can be written as:

$$\vec{r'} = \begin{pmatrix} 1+\frac{\epsilon}{2} & 0 \\ 0 & 1-\epsilon \end{pmatrix} \vec{r} \tag{2}$$

where $\vec{r}$ and $\vec{r'}$ are its initial and final orientations, respectively. The relation between the components of $\vec{r}$ and $\vec{r'}$ can be written as:

$$r_x = |\vec{r}|\cos\theta \qquad r_z = |\vec{r}|\sin\theta \qquad r'_x = |\vec{r'}|\cos\theta' \qquad r'_z = |\vec{r'}|\sin\theta' \tag{3}$$

where θ and θ' are the initial and the final angles between the crystal plane and the horizontal (fig. S2). Combining equations (2) and (3) we obtain:

$$\theta' = \arctan\left(\frac{1-\epsilon}{1+0.5\epsilon}\tan\theta\right) \tag{4}$$

This equation governs the rotation of mica crystals in response to vertical flattening.

Mica-group minerals are monoclinic (table S2), but their symmetry system can be treated as approximately hexagonal (2,3). For crystals with arbitrary orientations, the elastic tensor $c(\theta,\phi)$ can be computed by applying simple transformations of the fourth-order tensors:

$$c'_{nmop} = \beta_{ni}\beta_{mj}\beta_{ol}\beta_{pk}c_{ijlk} \tag{5}$$

where β is a rotation matrix. We consider an initial system with an isotropic orientation of mica crystals and apply transformation (4) to it. The resulting Voigt and Reuss averages of the elastic tensor become:

$$c_{voigt}(\epsilon) = \frac{1}{2\pi}\int_0^{2\pi}\int_0^{\pi/2} c\left(\arctan\left(\frac{1-\epsilon}{1+0.5\epsilon}\tan\theta\right),\phi\right)\sin\theta d\theta d\phi \tag{6}$$

$$c^{-1}_{reuss}(\epsilon) = \frac{1}{2\pi}\int_0^{2\pi}\int_0^{\pi/2} c^{-1}\left(\arctan\left(\frac{1-\epsilon}{1+0.5\epsilon}\tan\theta\right),\phi\right)\sin\theta d\theta d\phi \tag{7}$$

We solved equations (6) and (7) numerically for biotite and muscovite and, then, estimated Voigt and Reuss averages in a deformed aggregate composed of biotite and muscovite embedded into an isotropic matrix:

$$c_{voigt}(\epsilon) = a^{bio}c^{bio}_{voigt}(\epsilon) + a^{musc}c^{musc}_{voigt}(\epsilon) + a^{iso}c^{iso} \tag{8}$$

$$c^{-1}_{reuss}(\epsilon) = a^{bio}[c^{bio}_{reuss}(\epsilon)]^{-1} + a^{musc}[c^{musc}_{reuss}(\epsilon)]^{-1} + a^{iso}[c^{iso}]^{-1} \tag{9}$$

where a^{bio}, a^{musc}, and a^{iso} are volumetric fractions for biotite, muscovite and the isotropic matrix, respectively. Finally, we formed the Voigt-Russ-Hill average:

$$c(\epsilon) = \frac{1}{2}(c_{voigt}(\epsilon) + c_{reuss}(\epsilon)) \tag{10}$$

and used it to compute two shear wave velocities:

$$V_{SV}(\epsilon) = \sqrt{\frac{c_{2323}(\epsilon)}{\rho}} \tag{11}$$

$$V_{SH}(\epsilon) = \sqrt{\frac{c_{1212}(\epsilon)}{\rho}} \tag{12}$$

where ρ is density. In our computations, the density is 2850 kg/m^3 and the rigidity of the isotropic matrix is 42 GPa.

References

1. N.M. Shapiro, M.H. Ritzwoller, *Geophys. J. Int.* **151**, 88-105 (2002).
2. K.S. Aleksandrov, T.V. Ryzhova, *Izv. Acad. Nauk SSSR Ser. Geofiz.* **2**, 186-189 (1961).
3. O. Nishizawa, T. Yoshitno, *Geophys. J. Int.* **145**, 19-32 (2001).

Name	Monotonic constraint	P-to-S ratio	Parameters	Average misfit (m/s)
Isotropic monotonic	Yes	free	v_s^U, v_s^M, v_s^L, v_p^U, v_p^M, v_p^L	66.05
Isotropic	No	free	v_s^U, v_s^M, v_s^L, v_p^U, v_p^M, v_p^L	62.55
Anisotropic upper crust	Yes for isotropic v_s	fixed	v_s^M, v_s^L, v_{sv}^U, v_{sh}^U	57.25
Anisotropic middle crust	Yes for isotropic v_s	fixed	v_s^U, v_s^L, v_{sv}^M, v_{sh}^M	32.78
Anisotropic lower crust	Yes for isotropic v_s	fixed	v_s^U, v_s^M, v_{sv}^L, v_{sh}^L	52.83

Table S1. Parameterizations of the Tibetan crust tested in this paper. Last column shows the average group velocity misfit at periods below 50 s computed across the Tibetan region (in a square [28°N, 76°E; 38°N, 102°E]). Superscripts U, M, and L denote upper-crustal, mid-crustal, and lower-crustal values, respectively.

Mineral	c_{1111}	c_{3333}	c_{2323}	c_{1212}	c_{1133}
biotite	186.0	54.0	5.8	76.8	11.6
muscovite	178.0	54.9	12.2	67.8	14.5

Table S2. Elastic constants for minerals of the mica group (units are GPa).

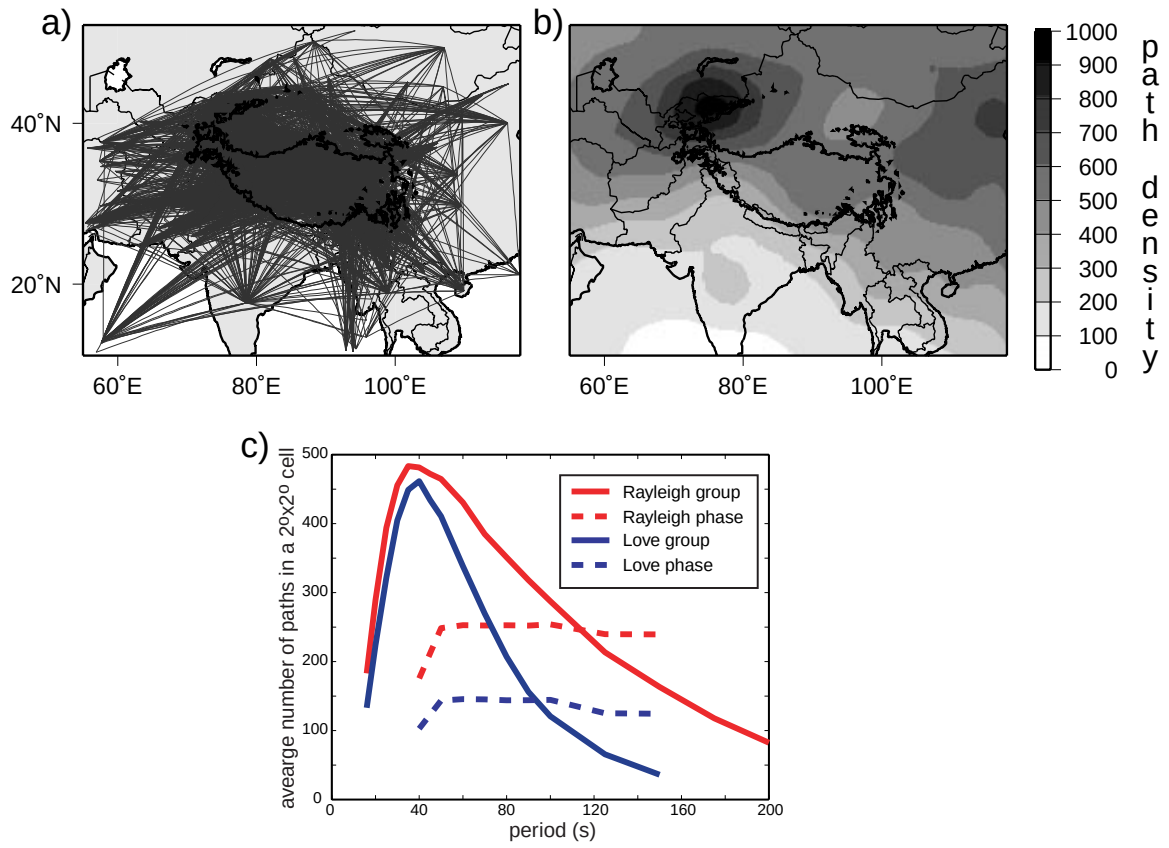

Fig. S1. Surface wave coverage. (a) Regional paths: approximately 3,000 regional surface-wave paths for which we measured dispersion curves at periods ∼40 s begin and end within the map shown. (b) Total path density (regional + teleseismic paths): more than 45,000 surface wave rays traverse a part of this region. Path density is defined as the number of rays crossing each $2^\circ \times 2^\circ$ cell. (c) Path density as a function of period for group and phase speeds of Love and Rayleigh waves.

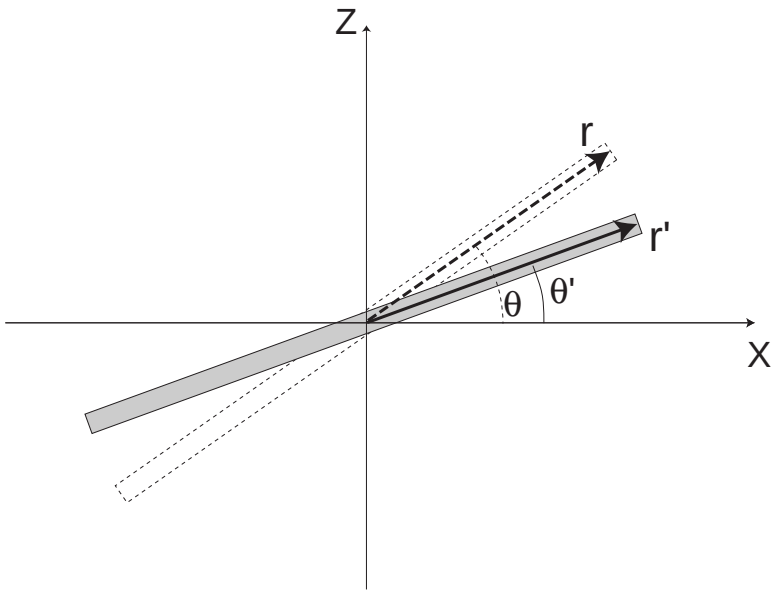

Fig. S2. Illustration of the two-dimensional rotation of an individual mica crystal where $\vec{r}$ and $\vec{r'}$ are its initial and final orientations, respectively, θ and θ' are initial and final angles between the crystal plane and the horizontal.